Upsala Journal of Medical Sciences

ISSN: 0300-9734 (Print) 2000-1967 (Online) Journal homepage: informahealthcare.com/journals/iups20

# Autoradiography screening of potential positron emission tomography tracers for asymptomatic abdominal aortic aneurysms

Gustaf Tegler, Sergio Estrada, Håkan Hall, Anders Wanhainen, Martin Björck, Jens Sörensen & Gunnar Antoni

**To cite this article:** Gustaf Tegler, Sergio Estrada, Håkan Hall, Anders Wanhainen, Martin Björck, Jens Sörensen & Gunnar Antoni (2014) Autoradiography screening of potential positron emission tomography tracers for asymptomatic abdominal aortic aneurysms, Upsala Journal of Medical Sciences, 119:3, 229-235, DOI: 10.3109/03009734.2014.894157

**To link to this article:** https://doi.org/10.3109/03009734.2014.894157

*Upsala Journal of Medical Sciences.* 2014; 119: 229–235

informa
healthcare

**ORIGINAL ARTICLE**

# Autoradiography screening of potential positron emission tomography tracers for asymptomatic abdominal aortic aneurysms

GUSTAF TEGLER[1], SERGIO ESTRADA[2], HÅKAN HALL[2], ANDERS WANHAINEN[1], MARTIN BJÖRCK[1], JENS SÖRENSEN[3,4] & GUNNAR ANTONI[2,4]

[1]*Department of Surgical Sciences, Section of Vascular Surgery, Uppsala University, Uppsala, Sweden,* [2]*Platform for Preclinical PET, Department of Medicinal Chemistry, Uppsala University, Uppsala, Sweden,* [3]*Nuclear Medicine and PET, Department of Radiology and Oncology and Radiation Sciences, Uppsala University, Uppsala, Sweden, and* [4]*PET Centre, Uppsala University, Uppsala, Sweden*

**Abstract**

*Objective.* The aetiology and early pathophysiological mechanisms of aortic aneurysm formation are still unknown and challenging to study *in vivo*. Positron emission tomography (PET) is a potentially valuable instrument for non-invasive *in vivo* pathophysiological studies. No specific tracer to identify the pathophysiological process of aneurysmal dilatation is yet available, however. The aim of this study was to explore if different PET tracers could be useful to image aneurysmal disease.

*Methods and results.* Human aneurysmal aortic tissue, collected during elective resection of abdominal aortic aneurysm (AAA) of asymptomatic patients, was investigated *in vitro* by means of autoradiography with [$^{68}$Ga]CRP-binder targeting C-reactive protein, [$^{11}$C]DAA1106 targeting translocator protein (18 kDa), [$^{11}$C]D-deprenyl with unknown target receptor, [$^{11}$C] deuterium-L-deprenyl targeting astrocytes, [$^{18}$F]fluciclatide targeting integrin $\alpha_V\beta_3$, [$^{68}$Ga]IMP461 and bi-specific antibody TF2 052107 targeting carcinoembryonic antigen, [$^{18}$F]F-metomidate targeting mitochondrial cytochrome P-450 species in the adrenal cortex, and [$^{18}$F]vorozole targeting aromatase. Of the investigated tracers, only [$^{18}$F]fluciclatide exhibited specific binding, whereas the other PET tracers failed to show specific uptake in the investigated tissue and are probably not useful for the intended purpose.

*Conclusion.* It seems likely that $\alpha_V\beta_3$ integrin expression in AAA can be visualized with PET and that the $\alpha_V\beta_3$ selective tracer, [$^{18}$F]fluciclatide, may be suitable for *in vivo* molecular imaging of asymptomatic AAA. Additional evaluation of [$^{18}$F] fluciclatide and $\alpha_V\beta_3$ integrin expression in AAA will be performed *in vitro* as well as *in vivo*.

**Key words:** *[18F]fluciclatide, abdominal aortic aneurysm, autoradiography, inflammation, PET, positron emission tomography*

## Introduction

The aetiology of degenerative abdominal aortic aneurysm (AAA) is mostly unknown. One of the observed features of the arterial wall in aneurysmal disease is degradation of connective tissue in the media layer. An increased proteolytic activity of matrix metalloproteinase, responsible for the degeneration of elastic lamellae and extracellular matrix proteins, has been demonstrated (1,2). Another observed characteristic is a chronic inflammation with large amounts of inflammatory cells, T- and B-lymphocytes, as well as macrophages (3). Furthermore, an increased medial neovascularization at the aneurysm rupture edge has been demonstrated. With angiogenesis as the predominant form of neovascularization in atherosclerosis it can be hypothesized that this process leads to a concomitant increase of $\alpha_V\beta_3$ integrin expression (4,5). Thus, there are multiple potential molecular targets or pathophysiological

Correspondence: Gustaf Tegler, MD, Department of Surgical Sciences, Section of Vascular Surgery, Uppsala University, SE-751 85 Uppsala, Sweden. Fax: +46 0 18 611 45 08. E-mail: gustaf@tegler.se

*(Received 8 November 2013; accepted 10 February 2014)*

ISSN 0300-9734 print/ISSN 2000-1967 online 
DOI: 10.3109/03009734.2014.894157

processes that, together with a suitable biomarker, could be of diagnostic or prognostic value in the management of AAA patients.

Methods for studies of the early pathophysiology in AAA *in vivo* are scarce. At the end stages of the disorder, biopsies may be obtained during surgery for histological investigations. A non-invasive diagnostic method that could differentiate between stable or metabolically active AAA at risk of rupture, based on knowledge at a molecular level, instead of size, would be of significant scientific and potential clinical value.

Positron emission tomography (PET) is a diagnostic imaging tool that provides a possibility for studies of pathophysiological mechanisms *in vivo* at the molecular level without interfering with that process. Together with computed tomography (CT), providing anatomical characteristics, the combined use of PET/CT has become a valuable instrument in various clinical settings, as well as a powerful research tool.

The aim of this study was to identify one or several useful PET tracers for the study of asymptomatic AAAs.

## Methods

### *PET tracers*

A number of tracers, originally intended for use in other disorders, were evaluated *in vitro* by means of autoradiography. Due to the infiltrate with inflammatory cells found in AAA, tracers with different characteristics of this field were tested: [$^{68}$Ga]CRP-binder (CRPB), [$^{11}$C]DAA1106 (DAA), and [$^{11}$C]D-deprenyl (DDE). Since angiogenesis has been suggested as a possible cause of aneurysm formation [$^{18}$F]fluciclatide was tested as well. Some tracers that were developed at the PET centre were tested on AAA tissue even though the likelihood of the intended receptors to be found in AAA tissue was very small: L-[$^{11}$C] di-deuteriumdeprenyl (DED), TF2 052107 with [$^{68}$Ga]IMP461 (TF2-IMP), [$^{18}$F]fluorometomidate (FMTO), and [$^{18}$F]vorozole (FVOZ).

All tracers were radiolabelled on site at the PET centre, Uppsala University Hospital, according to published methods. Some of the tracers were selected based on the potential of overexpression of certain receptors or enzymes in AAA tissue compared with normal aorta. Other tracers were tested merely based on availability.

*[$^{68}$Ga]CRP-binder (CRPB)* (6) is a polypeptide with a phosphocholine group that has a moderate affinity to C-reactive protein (CRP) ($K_d$ = 5 μM) (7). CRP is a protein that responds to inflammation and infections and can be detected in plasma (8). With the radiolabelled polypeptide targeting CRP it was hypothesized that the tissue responsible for the inflammation can be visualized *in vivo*. It might also be that this protein is expressed in inflammatory parts of AAA affected tissue.

*[$^{11}$C]DAA1106 (DAA)* is a ligand targeting the translocator protein (18 kDa), TSPO, also known as a peripheral benzodiazepine receptor (PBR), which is expressed on macrophages (9,10). It can be expected that macrophages are found in higher amounts in AAA tissue than in normal aorta. It has also been shown to be expressed in the brain in a variety of conditions: after stroke (11), in multiple sclerotic plaques (10,12), in dementia (13), and in refractory epilepsy (14). DAA has a high affinity to TSPO ($K_d$ = 0.043 nM), which is an order of magnitude higher than the commonly used tracers [$^{11}$C] PK11195 (15,16) and [$^{11}$C]PBR28 (17).

*[$^{11}$C]D-deprenyl (DDE)* is the inactive isomer of [$^{11}$C] L-deprenyl and has an as yet unknown binding site, but has shown prospects in revealing different inflammatory states. Thus, it has been useful in the diagnosis of e.g. whiplash trauma and rheumatoid arthritis (18,19). Potentially, the unknown inflammatory-related binding site could also be expressed in AAA tissue.

*[$^{18}$F]Fluciclatide* (20) is an integrin receptor ligand, exhibiting high selectivity and affinity for $\alpha_V\beta_3$ ($K_d$ ~10 nM) (21). Integrin $\alpha_V\beta_3$, also known as vitronectin receptor, has been shown to be upregulated in angiogenesis (22,23). It is expressed on macrophages (24), where it seems to be a mere expression rather than being involved in their activation (25,26). Angiogenesis is a process expected to be upregulated in AAA (4) as well as in the vicinity of platelets (27), osteoclasts (28,29), endothelial cells (30), and malignant cells, such as in melanoma (31) and breast cancer (21).

*L-[$^{11}$C]Di-deuteriumdeprenyl (DED)* is an irreversible inhibitor of monoamine oxidase type B (MAO-B) with high affinity and specificity (32,33). The tracer has been di-deuteriated in order to reduce the affinity towards the enzyme and minimize the blood flow dependency of the compound (34,35). In the diagnosis of epilepsy, this PET tracer, targeting astrocytes, has been of great value (36,37). Additional investigations of astrocytic invasion in patients with Alzheimer's disease have been carried out with this tracer along with the amyloid-β-specific tracer [$^{11}$C] PIB (38,39).

*TF2-IMP* is a bi-specific antibody coupled to a hapten. The TF2 052107 is a combined pretargeting antibody for carcinoembryonic antigen (CEA), which has a specific target site for the [$^{68}$Ga]IMP461 (IMP) PET tracer (40). CEAs are produced during fetal development and are expressed in a variety of

carcinomas, and can therefore be used as a biomarker both in tissue and in blood in those patients. Blood levels of CEA may also be elevated in other cancer types. The antibody is used as a pretarget of CEA and is subsequently visualized by the labelled hapten. The hapten IMP461(NOTA-D-Ala-D-Lys(HSG)-D-Tyr-D-Lys (HSG)-NH2) was obtained from Immunomedics, Inc. (Morris Plains, NJ, USA).

*[$^{18}$F]Fluorometomidate (FMTO)* is an analogue to the more commonly used [$^{11}$C]metomidate. It is useful in the visualization of adrenal cortical masses such as incidentalomas, adenomas, and primary and metastatic cortical carcinomas (41–43).

*[$^{18}$F]Vorozole (FVOZ)*. Vorozole, 6-[(4-chlorophenyl) (1,2,4-triazol-1-yl)methyl]-1-methylbenzotriazole, is a selective and potent non-steroidal aromatase enzyme inhibitor (44). [$^{18}$F]Vorozole (45) is an analogue with similar affinity to aromatase ($K_d$ = 0.21 nM) (46), an enzyme that converts androgen to estrogens. Aromatase inhibitors are used in the treatment of postmenopausal women with early-stage or advanced hormone-sensitive breast cancer. It has previously been labelled with the radionuclide $^{11}$C and used for visualization of aromatase distribution in the brain, especially the amygdala (46–48).

### *Experimental design*

*Human AAA tissue:* The study was approved by the Regional Ethics Committee of Uppsala/Örebro (Dnr 2007/052). Three male patients operated on for asymptomatic AAA, aged 65, 68, and 74 years, were investigated. The AAA diameters were 52, 56, and 66 mm. Biopsies obtained from the anterior segment of the AAAs were 10 × 10 mm thick and consisted of the full thickness of the aortic vessel wall. They were embedded in Tissue-Tek® OCT™ Compound (Sakura Finetek, Alphen aan den Rijn, The Netherlands), immediately cryo-fixed on dry ice and isopentane in the operating room, and stored at –70°C.

*Tracer syntheses:* The tracers used were, apart from [$^{18}$F]fluciclatide, synthesized according to standard procedures at the PET Centre, Uppsala University Hospital. [$^{18}$F]Fluciclatide was synthesized according to an established method in a FASTlab and provided by Uppsala Imanet AB/GE Healthcare.

*Frozen tissue autoradiography:* Glass slides with sections of AAA tissue, 20–25 μm thick, were incubated in a buffer solution containing a known concentration of the radioligand, as well as with their blocking substances with the same concentration but including an excess of a blocking substance, for assessment of non-specific binding (Table I). After incubation, slides were washed in cold buffer followed by a brief wash in distilled water, dried, and exposed to phosphor imaging plates for at least three radionuclide half-lives. Non-blocked and blocked samples were exposed under the same plate. The plates were then scanned in a Phosphor Imager Model 400S using 100 μm pixel width (Molecular Dynamics, Sunnyvale, CA, USA), and the digital images were analysed using software ImageQuant 5.1 (Molecular Dynamics).

### *Image analysis*

Autoradiograms were analysed using ImageQuant, and regions of interest (ROIs) were drawn manually on the digital images, delineating the whole segment of aortic tissue. Average pixel values were calculated, and the specific binding was determined as the difference between uptake with radioligand alone and that in the presence of an excess of blocking compound.

## Results

Only [$^{18}$F]fluciclatide displayed specific uptake (Figure 1), i.e. 88% of the uptake was blocked by co-incubation with excess of unlabelled fluciclatide, whereas the other tracers, CRP-binder, DAA, DDE, DED, TF2-IMP, FMTO, and FVOZ, did not display any specific uptake.

## Discussion

The natural course of AAA is to expand gradually and increase in diameter in order eventually to rupture, with a mortality rate as high as 90% (49). The only parameter to determine the time of intervention today is the diameter, usually obtained with ultrasound investigations. In order to intervene at an early phase of the pathology further knowledge on the pathophysiology is needed.

With PET/CT technology pathophysiological processes at the molecular level can be detected *in vivo*, which makes it a potentially important research tool to elucidate the mostly unknown mechanisms behind aneurysmal disease. If these processes can be identified and imaged they could serve as a proof of concept when evaluating different interventions to prevent growth and rupture. It has previously been shown *in vivo* that the chronic inflammation observed in the wall of large asymptomatic AAAs does not have sufficient metabolic activity to be detectable by

Table I. The *in vitro* labelling conditions for the different tracers.

| Abbreviation | Tracer | Molecular target | Concentration | Specific displacer | Buffer | Pre-incubation | Incubation | Wash (on ice) |
|---|---|---|---|---|---|---|---|---|
| CRPB | [$^{68}$Ga]CRP-binder | C-reactive protein | 0.01 MBq/mL, 0.205 nM | Phosphocholine, 10 μM | Tris-HCl 0.05 M, pH 7.4 + BSA 0.2% + $MgCl_2$ 5 mM + bacitracin 50 mg/L | 10 min RT | 60 min, 37°C | 3 × 3 min |
| DAA | [$^{11}$C]DAA1106 | Translocator protein (18 kDa) | 3 nM | PK11195, 1 μM | Tris-HCl 0.05 M, pH 7.4 | – | 40 min, RT | 3 × 3 min |
| DDE | [$^{11}$C]D-deprenyl | Unknown target receptor | 10 nM | D-deprenyl, 1 μM | PBS + BSA, 1%, pH 7.4 | – | 40 min, 37°C | 3 × 3 min |
| DED | [$^{11}$C]-deuterium-L-deprenyl | Astrocytes | 10 nM | L-deprenyl, 10 μM | 10 min in PBS + BSA | 10 min RT | 40 min, 37°C | 3 × 3 min |
| [$^{18}$F]fluciclatide | [$^{18}$F]fluciclatide | Integrin $\alpha_v\beta_3$ | 13 nM | Fluciclatide, 0.56 μM | Tris-HCl 0.05 M, pH 7.4 | 10 min RT | 60 min, RT | 3 × 3 min |
| TF2-IMP | [$^{68}$Ga]IMP461 and bi-specific antibody TF2 052107 | Carcinoembryonic antigen | 0.25 MBq/mL | No antibody | Tris-HCl 0.05 M, pH 7.4, + BSA 0.2% + $MgCl_2$ 5 mM + bacitracin 50 mg/L | 60 min at 37°C with TF2, wash 2×2 min wash on ice | 60 min, 37°C | 2 × 3 min |
| FMTO | [$^{18}$F]F-metomidate | Mitochondrial cytochrome P-450 species in the adrenal cortex | 0.007 MBq/mL | F-metomidate, 1 μM | Tris-HCl 0.05 M, pH 7.4 | 25 min, RT | 40 min, RT | 3 × 3 min |
| FVOZ | [$^{18}$F]vorozole | Aromatase | 0.1 MBq/mL, 2 nM | Vorozole, 1 μM | Tris-HCl 0.05 M, pH 7.4 | 10 min, RT | 30 min, RT | 3 × 2 min |

BSA = bovine serum albumin; HCl = hydrochloric acid; M = molar; MBq = megabecquerel; nM = nanomolar; PBS = phosphate-buffered saline; RT = room temperature; Tris = tris(hydroxymethyl)aminomethane; μM = micromolar.

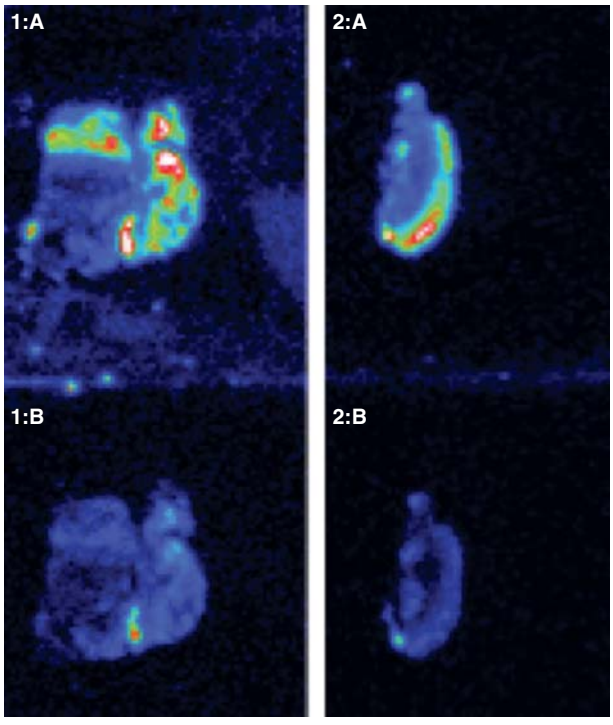


Figure 1. Autoradiography with [$^{18}$F]fluciclatide on AAA tissue from two patients. A: without additional blocking agent; and B: with additional blocking agent (unmarked fluciclatide).

[$^{18}$F]-fluorodeoxyglucose (FDG) PET, [$^{11}$C] PK11195, or [$^{11}$C]D-deprenyl (50-52). This was also verified in this *in vitro* study, as neither [$^{11}$C] DAA1106 nor [$^{11}$C]DDE showed any substantial binding to AAA tissue.

A limitation of the study is that some of the tested tracers were designed for a totally different specific target, e.g. TF2-IMP. Even though there are no clear indications of CEA receptors in AAA, we found it interesting to test them in an exploratory fashion. The fact that CRPB has such a low affinity ($K_d$ = 5 μM) might be the cause of the negative results. Thus, there might be CRP receptors in the tissue, although at a too low a concentration to be detectable. CRP has previously been found by immunohistochemical means in smooth muscle cells, foam cells, and macrophages in arteriosclerotic aortas (53). Until a CRPB tracer with higher affinity has been developed it is, however, not possible to use CRP as an *in vivo* target for use in AAA patients.

Macrophages are known to be present in AAA tissue, and as [$^{11}$C]DAA is a TSPO tracer it might be anticipated that this tracer is a good candidate for visualizing AAA. We have previously shown that the [$^{11}$C]PK11195 is not capable of detecting the TSPO receptor *in vivo* in patients with asymptomatic AAAs (52), but even though [$^{11}$C]DAA has higher affinity than [$^{11}$C]PK11195, it was not possible to visualize TSPO in AAA with [$^{11}$C]DAA. To our knowledge no immunohistochemical analysis for detection of TSPO antibody on AAA has been performed. It would be of great interest to investigate a TSPO tracer with even higher affinity than [$^{11}$C]DAA.

DDE is a tracer with an as yet unknown target receptor, but it has previously been shown to signal for chronic inflammation *in vivo* (18,19). However, the inflammation in AAA tissue is not active enough for the DDE tracer to become sufficiently taken up.

The DED tracer targets astrocytes, which has been useful in diagnosing Alzheimer's disease (38) and epilepsy (36,37), while TF2-IMP signals for CEA (40). FMTO visualizes adrenal cortical tumours (41–43), and FVOZ targets the enzyme aromatase (44). The likelihood is low that AAA tissue would have receptors for astrocytes, CEA, mitochondrial cytochrome P-450 species found in the adrenal cortex, or aromatase, but it cannot be entirely ruled out. The fact that these tracers (DED, TF2-IMP, FMTO, and FVOZ) did not signal in AAA tissue makes it unlikely that they are suitable for imaging of the pathophysiological processes of asymptomatic aneurysmal dilatation, at least in their current forms.

There was a substantial specific uptake of [$^{18}$F] fluciclatide, which targets the integrin $\alpha_V\beta_3$, an indicator for angiogenesis. Pathological processes in the *vasa vasorum* and angiogenesis as a cause of AAA formation have previously been suggested (54), and the increase of neovascularization has been demonstrated with immunohistochemical methods (55). With a PET tracer targeting integrin $\alpha_V\beta_3$ it might be possible to show an increased angiogenesis *in vivo*. It would then be of interest to study patients with small AAAs and thus to investigate a possible role of changed angiogenetic activities in the formation of AAA.

## Conclusion

The integrin-specific tracer [$^{18}$F]fluciclatide might be useful in the detection of angiogenesis in asymptomatic AAAs. Further *in vivo* molecular imaging studies of asymptomatic AAAs with [$^{18}$F]fluciclatide are warranted, and additional *in vitro* studies of novel PET tracers may reveal new imaging possibilities.

## Acknowledgements

We are most grateful to Associate Professor Irina Velikyan, Obaidur Rahman, PhD, and Maria Erlandsson, PhD, for synthesis of DDE, DAA, DED, FVOZ, FMTO, TF2-IMP, and CRPB, which made this study possible. Professor Bengt Långström is acknowledged for his valuable input. We also thank

Uppsala Imanet AB and GE Healthcare for granting access to the use of the tracer [$^{18}$F]fluciclatide.

***Declaration of interest:*** The study was funded by the Swedish Research Council (Grant K2013-64X-20406-07-3) and an Amersham research grant. The authors report no conflicts of interest. The authors alone are responsible for the content and writing of the paper.

## References

1. Tamarina NA, McMillan WD, Shively VP, Pearce WH. Expression of matrix metalloproteinases and their inhibitors in aneurysms and normal aorta. Surgery. 1997;122:264–71.
2. Kadoglou NP, Liapis CD. Matrix metalloproteinases: contribution to pathogenesis, diagnosis, surveillance and treatment of abdominal aortic aneurysms. Curr Med Res Opin. 2004;20:419–32.
3. Jacob T, Ascher E, Hingorani A, Gunduz Y, Kallakuri S. Initial steps in the unifying theory of the pathogenesis of artery aneurysms. J Surg Res. 2001;101:37–43.
4. Choke E, Thompson MM, Dawson J, Wilson WR, Sayed S, Loftus IM, et al. Abdominal aortic aneurysm rupture is associated with increased medial neovascularization and overexpression of proangiogenic cytokines. Arterioscler Thromb Vasc Biol. 2006;26:2077–82.
5. Lin S-A, Patel M, Suresch D, Connolly B, Bao B, Groves K, et al. Quantitative longitudinal imaging of vascular inflammation and treatment by ezetimibe in apoE mice by FMT using new optical imaging biomarkers of cathepsin activity and integrin. Int J Mol Imaging. 2012;2012:189254.
6. Blom E. Development of 18F- and 68Ga-labelled tracers: design perspectives and the search for faster synthesis. University of Uppsala, Sweden: Acta Universitatis Upsaliensis; 2009.
7. Christopeit T, Gossas T, Danielson UH. Characterization of $Ca^{2+}$ and phosphocholine interactions with C-reactive protein using a surface plasmon resonance biosensor. Anal Biochem. 2009;391:39–44.
8. Black S, Kushner I, Samols D. C-reactive protein. J Biol Chem. 2004;279:48487–90.
9. Zavala F, Haumont J, Lenfant M. Interaction of benzodiazepines with mouse macrophages. Eur J Pharmacol. 1984;106:561–6.
10. Vowinckel E, Reutens D, Becher B, Verge G, Evans A, Owens T, et al. PK11195 binding to the peripheral benzodiazepine receptor as a marker of microglia activation in multiple sclerosis and experimental autoimmune encephalomyelitis. J Neurosci Res. 1997;50:345–53.
11. Pappata S, Levasseur M, Gunn RN, Myers R, Crouzel C, Syrota A, et al. Thalamic microglial activation in ischemic stroke detected in vivo by PET and [$^{11}$C]PK1195. Neurology. 2000;55:1052–4.
12. Banati RB, Newcombe J, Gunn RN, Cagnin A, Turkheimer F, Heppner F, et al. The peripheral benzodiazepine binding site in the brain in multiple sclerosis: quantitative in vivo imaging of microglia as a measure of disease activity. Brain. 2000;123:2321–37.
13. Cagnin A, Brooks DJ, Kennedy AM, Gunn RN, Myers R, Turkheimer FE, et al. In-vivo measurement of activated microglia in dementia. Lancet. 2001;358:461–7.
14. Goerres GW, Revesz T, Duncan J, Banati RB. Imaging cerebral vasculitis in refractory epilepsy using [$^{11}$C](R)-PK11195 positron emission tomography. AJR Am J Roentgenol. 2001;176:1016–18.
15. Maeda J, Suhara T, Zhang MR, Okauchi T, Yasuno F, Ikoma Y, et al. Novel peripheral benzodiazepine receptor ligand [$^{11}$C]DAA1106 for PET: an imaging tool for glial cells in the brain. Synapse. 2004;52:283–91.
16. Pugliese F, Gaemperli O, Kinderlerer AR, Lamare F, Shalhoub J, Davies AH, et al. Imaging of vascular inflammation with [$^{11}$C]-PK11195 and positron emission tomography/computed tomography angiography. J Am Coll Cardiol. 2010;56:653–61.
17. Owen DRJ, Gunn RN, Rabiner EA, Bennacef I, Fujita M, Kreisl WC, et al. Mixed-affinity binding in humans with 18-kDa translocator protein ligands. J Nucl Med. 2011;52:24–32.
18. Danfors T, Bergström M, Feltelius N, Ahlström H, Westerberg G, Långström B. Positron emission tomography with $^{11}$C-D-Deprenyl in patients with rheumatoid arthritis. Evaluation of knee joint inflammation before and after intraarticular glucocorticoid treatment. Scand J Rheumatol. 1997;26:43–8.
19. Linnman C, Appel L, Fredrikson M, Gordh T, Söderlund A, Långström B, et al. Elevated [$^{11}$C]-D-deprenyl uptake in chronic whiplash associated disorder suggests persistent musculoskeletal inflammation. PLoS One. 2011;6:e19182.
20. Glaser M, Morrison M, Solbakken M, Arukwe J, Karlsen H, Wiggen U, et al. Radiosynthesis and biodistribution of cyclic RGD peptides conjugated with novel [$^{18}$F]fluorinated aldehyde-containing prosthetic groups. Bioconjug Chem. 2008;19:951–7.
21. Kenny LM, Coombes RC, Oulie I, Contractor KB, Miller M, Spinks TJ, et al. Phase I trial of the positron-emitting Arg-Gly-Asp (RGD) peptide radioligand $^{18}$F-AH111585 in breast cancer patients. J Nucl Med. 2008;49:879–86.
22. Morrison MS, Ricketts SA, Barnett J, Cuthbertson A, Tessier J, Wedge SR. Use of a novel Arg-Gly-Asp Radioligand, $^{18}$F-AH111585, to determine changes in tumor vascularity after antitumor therapy. J Nucl Med. 2009;50:116–22.
23. Brooks PC, Clark RA, Cheresh DA. Requirement of vascular integrin αVβ3 for angiogenesis. Science. 1994;264:569–71.
24. Bishop GG, McPherson JA, Sanders JM, Hesselbacher SE, Feldman MJ, McNamara CA, et al. Selective αvβ3-receptor blockade reduces macrophage infiltration and restenosis after balloon angioplasty in the atherosclerotic rabbit. Circulation. 2001;103:1906–11.
25. Gordon S. Alternative activation of macrophages. Nat Rev Immunol. 2003;3:23–35.
26. Antonov AS, Kolodgie FD, Munn DH, Gerrity RG. Regulation of macrophage foam cell formation by αVβ3 integrin: potential role in human atherosclerosis. Am J Pathol. 2004;165:247–58.
27. Coller BS, Cheresh DA, Asch E, Seligsohn U. Platelet vitronectin receptor expression differentiates Iraqi-Jewish from arab patients with Glanzmann thrombasthenia in Israel. Blood. 1991;77:75–83.
28. Zheleznyak A, Wadas T, Sherman C, Wilson J, Kostenuik P, Weilbaecher K, et al. Integrin αvβ3 as a PET imaging biomarker for osteoclast number in mouse models of negative and positive osteoclast regulation. Mol Imaging Biol. 2012;14:500–8.
29. Horton MA. The αvβ3 integrin vitronectin receptor. Int J Biochem Cell Biol. 1997;29:721–5.
30. Conforti G, Dominguez-Jimenez C, Zanetti A, Gimbrone MA Jr, Cremona O, Marchisio PC, et al. Human

endothelial cells express integrin receptors on the luminal aspect of their membrane. Blood. 1992;80:437–46.
31. Montgomery AM, Reisfeld RA, Cheresh DA. Integrin αvβ3 rescues melanoma cells from apoptosis in three-dimensional dermal collagen. Proc Natl Acad Sci USA. 1994;91:8856–60.
32. Fowler JS, Logan J, Volkow ND, Wang GJ. Translational neuroimaging: positron emission tomography studies of monoamine oxidase. Mol Imaging Biol. 2005;7:377–87.
33. Fowler JS, MacGregor RR, Wolf AP, Arnett CD, Dewey SL, Schlyer D, et al. Mapping human brain monoamine oxidase A and B with $^{11}$C-labeled suicide inactivators and PET. Science. 1987;235:481–5.
34. MacGregor RR, Fowler JS, Wolf AP, Halldin C, Långström B. Synthesis of suicide inhibitors of monoamine oxidase: carbon-11 labeled clorgyline, L-deprenyl and D-deprenyl. J Labelled Comp Radiopharm. 1988;25:1–9.
35. Fowler JS, Wang GJ, Logan J, Xie S, Volkow ND, MacGregor RR, et al. Selective reduction of radiotracer trapping by deuterium substitution: comparison of carbon-11-L-Deprenyl and carbon-11-Deprenyl-D2 for MAO B mapping. J Nucl Med. 1995;36:1255–62.
36. Kumlien E, Bergström M, Lilja A, Andersson J, Szekeres V, Westerberg CE, et al. Positron emission tomography with $^{11}$C-deuterium-deprenyl in temporal lobe epilepsy. Epilepsia. 1995;36:712–21.
37. Kumlien E, Nilsson A, Hagberg G, Långström B, Bergström M. PET with $^{11}$C-deuterium-deprenyl and $^{18}$F-FDG in focal epilepsy. Acta Neurol Scand. 2001;103: 360–6.
38. Carter SF, Schöll M, Almkvist O, Wall A, Engler H, Långström B, et al. Evidence for astrocytosis in prodromal alzheimer disease provided by $^{11}$C-Deuterium-L-Deprenyl: a multitracer PET paradigm combining $^{11}$C-Pittsburgh compound B and $^{18}$F-FDG. J Nucl Med. 2012;53:37–46.
39. Klunk WE, Engler H, Nordberg A, Wang Y, Blomqvist G, Holt DP, et al. Imaging brain amyloid in Alzheimer's disease with Pittsburgh compound-B. Ann Neurol. 2004;55:306–19.
40. Hall H, Velikyan I, Blom E, Ulin J, Monazzam A, Påhlman L, et al. In vitro autoradiography of carcinoembryonic antigen in tissue from patients with colorectal cancer using multifunctional antibody TF2 and $^{67/68}$Ga-labeled haptens by pretargeting. Am J Nucl Med Mol Imaging. 2012;2:141–50.
41. Bergström M, Bonasera TA, Lu L, Bergström E, Backlin C, Juhlin C, et al. In vitro and in vivo primate evaluation of carbon-11-etomidate and carbon-11-metomidate as potential tracers for PET imaging of the adrenal cortex and its tumors. J Nucl Med. 1998;39:982–9.
42. Erlandsson M, Karimi F, Lindhe Ö, Långström B. $^{18}$F-Labelled metomidate analogues as adrenocortical imaging agents. Nucl Med Biol. 2009;36:435–45.
43. Ettlinger DE, Wadsak W, Mien LK, Machek M, Wabnegger L, Rendl G, et al. [$^{18}$F]FETO: metabolic considerations. Eur J Nucl Med Mol Imaging. 2006;33:928–31.
44. Wouters W, Van Ginckel R, Krekels M, Bowden C, De Coster R. Pharmacology of vorozole. J Steroid Biochem Mol Biol. 1993;44:617–21.
45. Erlandsson M, Karimi F, Takahashi K, Långström B. $^{18}$F-Labelled vorozole analogues as PET tracer for aromatase. J Labelled Comp Radiopharm. 2008;51:207–12.
46. Hall H, Takahashi K, Erlandsson M, Estrada S, Razifar P, Bergström E, et al. Pharmacological characterization of $^{18}$F-labeled vorozole analogs. J Labelled Comp Radiopharm. 2012;55:484–90.
47. Takahashi K, Bergström M, Frändberg P, Vesström EL, Watanabe Y, Långström B. Imaging of aromatase distribution in rat and rhesus monkey brains with [$^{11}$C]vorozole. Nucl Med Biol. 2006;33:599–605.
48. Lidström P, Bonasera TA, Kirilovas D, Lindblom B, Lu L, Bergström E, et al. Synthesis, in vivo rhesus monkey biodistribution and in vitro evaluation of a $^{11}$C-labelled potent aromatase inhibitor: [N-methyl-$^{11}$C]vorozole. Nucl Med Biol. 1998;25:497–501.
49. Bengtsson H, Bergqvist D. Ruptured abdominal aortic aneurysm: a population-based study. J Vasc Surg. 1993;18: 74–80.
50. Tegler G, Ericson K, Sörensen J, Björck M, Wanhainen A. Inflammation in the walls of asymptomatic abdominal aortic aneurysms is not associated with increased metabolic activity detectable by 18-fluorodeoxglucose positron-emission tomography. J Vasc Surg. 2012;56:802–7.
51. Palombo D, Morbelli S, Spinella G, Pane B, Marini C, Rousas N, et al. A positron emission tomography/computed tomography (PET/CT) evaluation of asymptomatic abdominal aortic aneurysms: another point of view. Ann Vasc Surg. 2012;26:491–9.
52. Tegler G, Sörensen J, Ericson K, Björck M, Wanhainen A. 4D-PET/CT with [$^{11}$C]-PK11195 and [$^{11}$C]-D-deprenyl does not identify the chronic inflammation in asymptomatic abdominal aortic aneurysms. Eur J Vasc Endovasc Surg. 2013; 45:351–6.
53. Hatanaka K, Li X-A, Masuda K, Yutani C, Yamamoto A. Immunohistochemical localization of C-reactive protein-binding sites in human atherosclerotic aortic lesions by a modified streptavidin-biotin-staining method. Pathol Int. 1995;45:635–41.
54. Benjamin HB, Bartenbach G, Zeit W. The importance of the vasa vasorum of the aorta. Surg Gynecol Obstet. 1960;110: 224–8.
55. Paik DC, Fu C, Bhattacharya J, Tilson MD. Ongoing angiogenesis in blood vessels of the abdominal aortic aneurysm. Exp Mol Med. 2004;36:524–33.